nature geoscience

ARTICLES

PUBLISHED ONLINE: 24 FEBRUARY 2013 | DOI: 10.1038/NGEO1738

Antarctic Bottom Water production by intense sea-ice formation in the Cape Darnley polynya

Kay I. Ohshima[1]*†, Yasushi Fukamachi[1]†, Guy D. Williams[2]†, Sohey Nihashi[3], Fabien Roquet[4], Yujiro Kitade[5], Takeshi Tamura[6], Daisuke Hirano[5], Laura Herraiz-Borreguero[2], Iain Field[7], Mark Hindell[8], Shigeru Aoki[1] and Masaaki Wakatsuchi[1]

The formation of Antarctic Bottom Water—the cold, dense water that occupies the abyssal layer of the global ocean—is a key process in global ocean circulation. This water mass is formed as dense shelf water sinks to depth. Three regions around Antarctica where this process takes place have been previously documented. The presence of another source has been identified in hydrographic and tracer data, although the site of formation is not well constrained. Here we document the formation of dense shelf water in the Cape Darnley polynya (65°–69° E) and its subsequent transformation into bottom water using data from moorings and instrumented elephant seals (*Mirounga leonina*). Unlike the previously identified sources of Antarctic Bottom Water, which require the presence of an ice shelf or a large storage volume, bottom water production at the Cape Darnley polynya is driven primarily by the flux of salt released by sea-ice formation. We estimate that about 0.3–0.7 × 10^6 m^3 s^{-1} of dense shelf water produced by the Cape Darnley polynya is transformed into Antarctic Bottom Water. The transformation of this water mass, which we term Cape Darnley Bottom Water, accounts for 6–13% of the circumpolar total.

Antarctic bottom water (AABW) is the cold, dense water in the abyssal layer, accounting for 30–40% of the global ocean mass[1]. AABW production is a major contributor to the global overturning circulation[1–3] and represents an important sink for heat and possibly CO_2 (ref. 4). AABW originates as dense shelf water (DSW), which forms on the continental shelf by regionally varying combinations of brine rejection from sea-ice growth and ocean/ice-shelf interactions. With sufficient negative buoyancy and an export pathway across the shelf break, the DSW can mix down the continental slope with ambient water masses to produce AABW (ref. 5). At present, AABW production is recognized in three main regions: the Weddell Sea[6–9], the Ross Sea[10–12] and off the Adélie Coast[13–15] (Fig. 1, inset map). In the Weddell and Ross seas, large continental embayments associated with major continental ice shelves were considered necessary mechanisms to generate sufficient negative buoyancy in local DSW for the production of AABW (refs 9,10). This paradigm was broken when Adélie Land Bottom Water was directly linked to coastal polynyas, thin ice areas of enhanced sea-ice production and associated brine rejection. Although many polynya regions exist, particularly in East Antarctica, the storage capacity of the continental shelf in this region was proposed as the reason this seemed to be the only polynya region capable of forming sufficiently saline DSW for producing AABW (refs 14,15).

Another independent variety of AABW, previously identified in the Weddell–Enderby Basin (Fig. 1, inset map) from offshore properties detailed in hydrographic and tracer studies[16–21], has presented a puzzle in terms of its existence and DSW source. The Prydz Bay region (71°–80° E) seemed the most likely candidate[22–24], with its large continental embayment and the presence of the Amery Ice Shelf resembling the Weddell Sea and Ross Sea AABW regions. However, the results from several ship-based studies[21] were inconclusive and the export of DSW and its downslope transport were never observed from this region.

Most recently, satellite-derived estimates of sea-ice production suggest that the Cape Darnley polynya (CDP), located northwest of the Amery Ice Shelf (Fig. 1), has the second highest ice production around Antarctica after the Ross Sea Polynya[25]. This satellite analysis provided the motivation for an extensive Japanese mooring programme conducted in 2008–2009 as part of the International Polar Year, to prove the production of AABW from the CDP. Here we present the successful results of the moorings and observations of new AABW on the continental slope off the CDP. Furthermore, we confirm that the CDP is the DSW source for this AABW based on instrumented seal data, which has recently become an important source of hydrographic profiles in logistically challenging regions/seasons around the Antarctic margin[26–28]. Finally, the contribution of this AABW to total AABW is discussed.

Intense sea-ice production in the polynya

A new high-resolution satellite data set is used here to enhance understanding of the CDP from previous studies[25,29,30]. A typical synthetic aperture radar image of the CDP (Fig. 1) clearly reveals the extent of the CDP (>10^4 km^2), in which the newly formed sea ice appears as white streaks (high radar backscatter). The annual ice-production estimate from the Advanced Microwave Scanning Radiometer-EOS (AMSR-E) data (Supplementary Section S1) details the extremely high ice production of 195 ± 71 km^3, with

[1]Institute of Low Temperature Science, Hokkaido University, Sapporo 060-0819, Japan, [2]Antarctic Climate and Ecosystem Cooperative Research Centre, University of Tasmania, Hobart 7001, Australia, [3]Tomakomai National College of Technology, Tomakomai 059-1275, Japan, [4]Department of Meteorology, Stockholm University, S-106 91 Stockholm, Sweden, [5]Tokyo University of Marine Science and Technology, Tokyo 108-8477, Japan, [6]National Institute of Polar Research, Tachikawa 190-8518, Japan, [7]Graduate School of the Environment, Macquarie University, 2109, Australia, [8]Institute for Marine and Antarctic Studies, University of Tasmania, 7001, Australia. †These authors contributed equally to this work. *e-mail: ohshima@lowtem.hokudai.ac.jp.

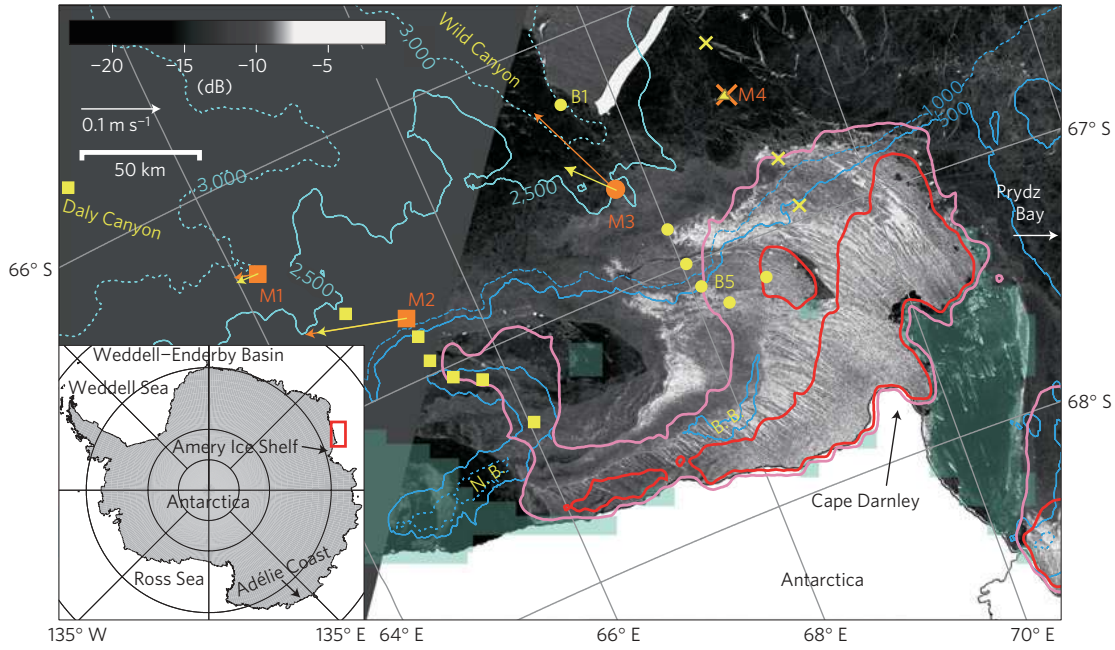

Figure 1 | Intense sea-ice production in the CDP, revealed from satellite data. The background ENVISAT ASAR image is from 7 August 2008. The black–white graded scale bar in the top left indicates the backscatter coefficient. Annual sea-ice production in 2008, estimated from the AMSR-E data, is indicated by red (>10 m yr^{-1}) and pink (>5 m yr^{-1}) contours. Fast ice areas, as detected by the AMSR-E algorithm, are highlighted in green. The bathymetry is indicated by blue contours. Mooring locations are indicated by orange symbols, with the mean velocity at the bottom and top of the mooring shown as orange and yellow vectors, respectively. CTD station lines A, B and C are denoted by squares, circles and crosses, respectively. The Nielsen (N.B.) and Burton (B.B.) basins are as shown. The inset map shows the location of the study area (red rectangle).

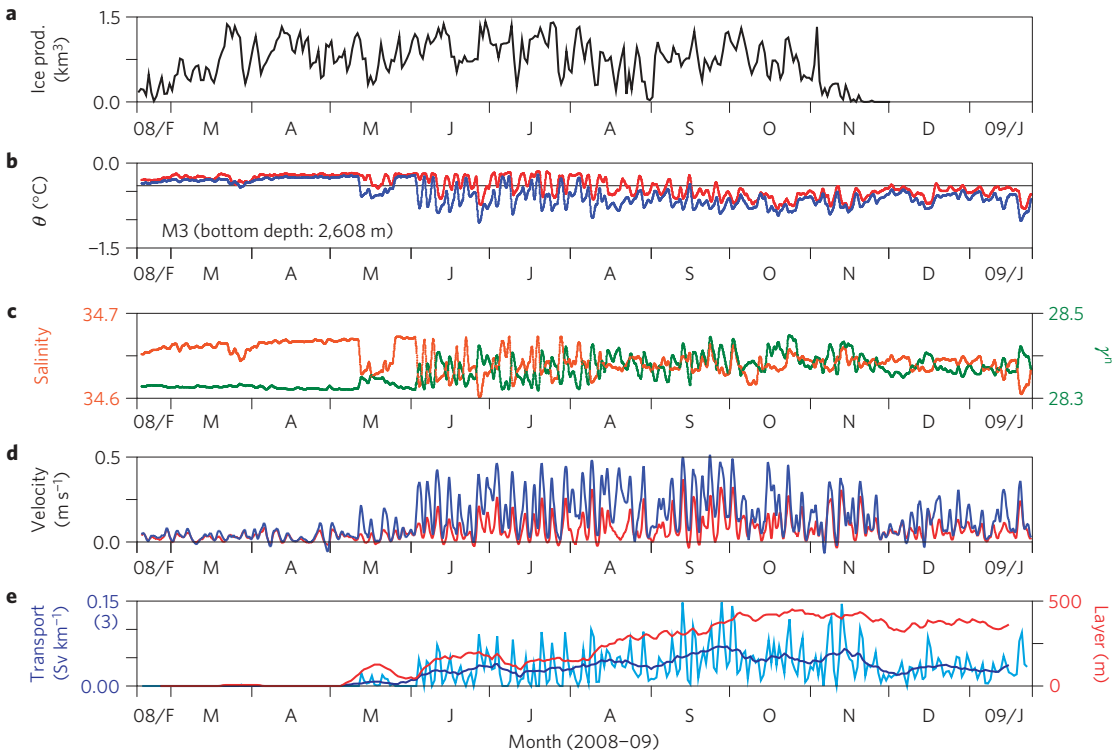

Figure 2 | Observations of new AABW production in Wild Canyon offshore from the CDP. a, Daily sea-ice production in the CDP estimated from AMSR-E data and a heat-flux calculation. **b**–**e**, M3 mooring time-series of potential temperature (θ) at depths of 26 m (blue) and 224 m (red) from the bottom (**b**), salinity (orange) and neutral density (γ^n, green) at 26 m from the bottom (**c**), the velocity component of the mean (dominant) flow direction at 20 m (blue) and 226 m (red) from the bottom (**d**) and the estimated layer thickness (red, 15-day running mean) and volume transport per unit width (light blue, daily mean; dark blue, 15-day running mean) of new AABW (**e**). The value in parentheses on the left axis shows the volume transport (Sv = 10^6 m^3 s^{-1}) for an assumed current width of 20 km in **e**.

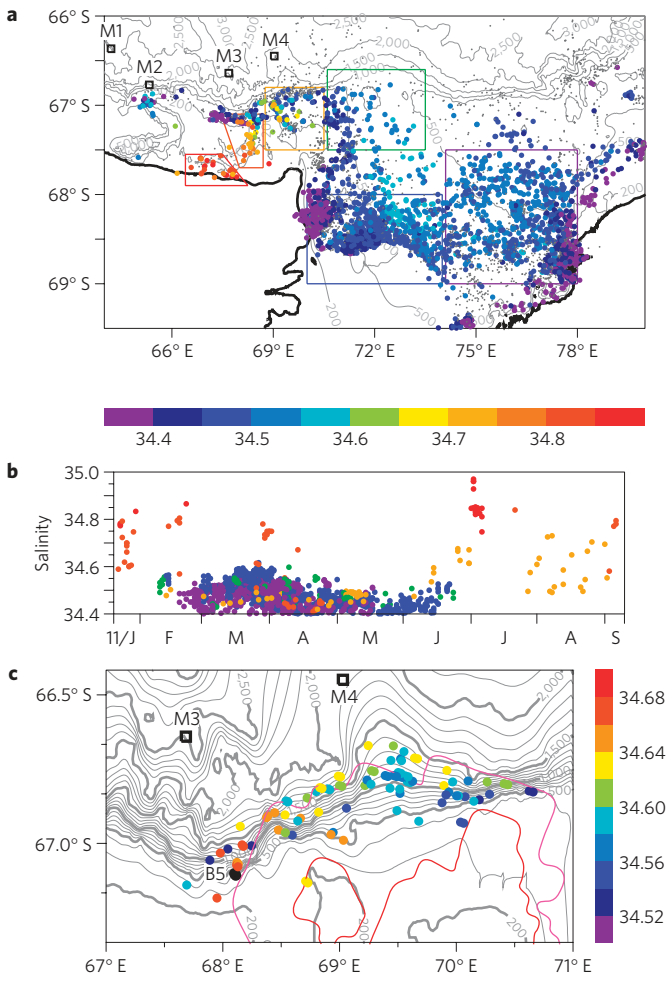

Figure 3 | Bottom salinities of DSW and mSW from the instrumented seals. a, Salinities of bottom-of-dive data for all available seal profiles with the bottom depth >250 m and potential temperature $\theta < -1.7$ °C over the continental shelf off Cape Darnley and in Prydz Bay. All other dive locations are indicated by small grey points. It is noted that, for these temperatures and depths, salinity >34.5 approximately corresponds to $\gamma^n > 28.27\,kg\,m^{-3}$, threshold of AABW density[2]. **b**, Spatial and temporal variation in salinities of bottom-of-dive data shown in **a**. Symbols follow those in **a**, coloured according to the regional outlines in **a**. **c**, Bottom salinities for overflows of mSW ($\theta < -0.8$ °C, bottom depth >800 m) in the region between 67° and 71° E. The annual sea-ice production is contoured as in Fig. 1.

local production rates exceeding $10\,m\,yr^{-1}$. The dark zone with small white patches just east of the polynya is a grounded iceberg tongue[30] (highlighted in green). With the prevailing ocean currents directed westward and dominant offshore winds, newly formed sea ice accumulates to the east of this barrier and is advected away to the west. This mechanism makes this polynya the second largest in area in the Antarctic, with a large associated salt flux (Supplementary Table S1).

New AABW production off the polynya

The moorings were deployed at four locations: at M1 (water depth: 2,923 m) and M3 (depth: 2,608 m) within the Daly and Wild canyons, predicted to be the DSW/AABW pathways, and at M2 (depth: 1,439 m) and M4 (depth: 1,824 m) over the continental slope (see Fig. 1 and Supplementary Table S2). M3, located at the centre of Wild Canyon just off the CDP, showed the most prominent downslope current (orange vector in Fig. 1). The mean flow was directed downslope, as determined by multi-beam bathymetry measurements during deployment, and had prominent bottom intensification (Fig. 1). In May, two months after the onset of active sea-ice production (Fig. 2a), a colder, less saline, and denser signal abruptly appeared at all instruments (up to 224 m from the bottom) and became dominant after June (Fig. 2b,c). The current speeds across this layer intensified in conjunction with the cold and dense signal (Fig. 2d). Thereafter, downslope current speeds of up to $0.5\,m\,s^{-1}$ fluctuated coherently with these water properties. Spectral analysis reveals strong peaks at periods of 4 and 5 days. The thickness of the cascading AABW layer was estimated by linear extrapolation to increase up to ~400 m from May to October and to remain >300 m to January (Fig. 2e and Supplementary Section S5a). With these properties (neutral density $\gamma^n > 28.27\,kg\,m^{-3}$) at this depth range (>2,500 m), these observations represent new AABW that would be within the range of AABW in the Weddell Sea[2] (Supplementary Fig. S8a).

We consider the observed downslope flows, with cold, dense properties and strong bottom intensification, to be gravity currents (Supplementary Section S2c). Together with analysis of a salinity budget estimated from the satellite data (Supplementary Section S6a), we propose that after two months of high sea-ice production in the CDP, the salinity and hence density of the shelf water is sufficient to descend the slope, channelled by the canyons. The fluctuating signal at M3 probably originates from a periodic outflow due to the baroclinic instability associated with the front between this DSW and the less dense ambient water offshore[31]. Thereafter, the DSW can descend in the form of an eddy or plume[5,31–33]. The cold dense water could descend to even greater depths with the aid of thermobaricity[9,34].

The moorings at M1, M2 and M4 also reported varying degrees of new AABW production. Cold and dense water was observed at moorings M1 and M2 shortly after the onset of active sea-ice production (Supplementary Fig. S3a–d). These data indicate that DSW from the CDP is initially just advected westwards along the slope (M2) and that new AABW is also transported down Daly Canyon (M1). A cold and dense signal was also found at M4 (Supplementary Fig. S3e,f) and possibly indicates the influence of DSW formed upstream of the CDP. However, the near-bottom signal is much thinner (Supplementary Fig. S5), suggesting that its contribution is minor relative to the CDP.

DSW revealed by the instrumented seals

Southern elephant seals (*Mirounga leonina*) equipped with conductivity–temperature–depth (CTD) sensors (Supplementary Section S4) reveal the spatial distribution and seasonal evolution of DSW properties over the continental shelf off Cape Darnley and to the east in Prydz Bay. Hydrographic data were post-processed using a set of delayed-mode techniques[35], yielding sufficient accuracies for the characterization of DSW, that is, about 0.03 °C in temperature and 0.05 or better in salinity. The bottom-of-dive salinity (Supplementary Section S4c) for all available seal profiles with bottom depth >250 m and potential temperature $\theta < -1.7$ °C is shown in Fig. 3a,b. The spatial distribution clearly reveals the high-salinity DSW over the CDP region (Fig. 3a), consistent with the high ice production (Fig. 1). We identify six regional subsets that cover the continental shelf in this region (Fig. 3a) and find the most saline DSW in the inshore region of the continental shelf west of Cape Darnley (red outline in Fig. 3a), with actively forming (late June through early July) and remnant (January–February) DSW salinities >34.8 (red data in Fig. 3b). These are among the most saline and therefore densest shelf waters observed around Antarctica[14,15,24,36,37]. This region overlaps with the high annual ice production of $>5\,m\,yr^{-1}$ (Fig. 1). In contrast, there

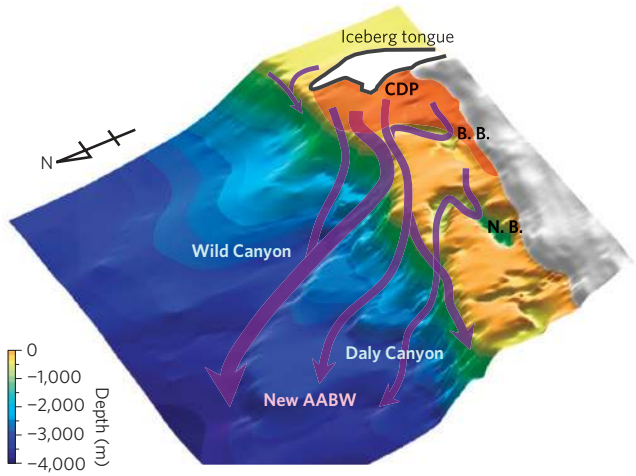

Figure 4 | Schematic of CDBW production. Enhanced sea-ice production (red shading) in the CDP formed leeside of the grounded iceberg tongue causes DSW formation through the high brine (salt) rejection. The downslope pathway from DSW to new AABW is represented by the purple arrows. The primary DSW descends down Wild Canyon. The remainder flows westwards over the shelf and slope with geostrophic balance and then downslope elsewhere in the west (mostly along Daly Canyon). DSW, through mixing with overlying CDW, is gradually transformed into new AABW (CDBW). B.B., Nielsen basin; N.B, Burton basin.

is a lower-salinity (34.5–34.6) variety of DSW observed over the Prydz Bay shelf from March to mid-June (green, blue and purple data in Fig. 3b).

Several of the instrumented seals foraged on the continental slope to depths as great as 1,800 m. These returned very rare wintertime measurements of overflowing DSW, also referred to as modified Shelf Water[15,37] (mSW), in the region just off CDP and southeast of M3, between 67.5° and 71.0° E. The bottom salinities from available profiles with strong mSW signatures (colder, fresher and denser relative to the ambient slope water, see Supplementary Fig. S6) are shown in Fig. 3c. The key feature here is the clear shift to more saline and denser (>34.64) bottom values from east to west, in particular west of ~68.5° E. These results, along with the mooring results, confirm that high-salinity DSW from the CDP region is the main source of the new AABW cascading down the canyons. Although there is likely to be some weak contribution or pre-conditioning by low-salinity DSW exported from Prydz Bay, it cannot be quantified at this point.

Implications of Cape Darnley Bottom Water production

Our discovery of new AABW production offshore from the CDP is a major missing piece of a 30-year-old puzzle regarding the source of recently ventilated AABW in the Weddell–Enderby Basin. We propose to name this AABW Cape Darnley Bottom Water (CDBW) and summarize its production schematically in Fig. 4. DSW produced in the CDP descends down Wild and Daly canyons and is transformed into CDBW through mixing with overlying Circumpolar Deep Water (CDW). On the basis of its observed properties, relative to the water masses reported in the Weddell Sea[18–20], CDBW should migrate further westward, and increase its volume by gradual mixing with CDW, to ultimately constitute part of the AABW in the Weddell Sea referred to as Weddell Sea Deep Water (WSDW).

We now investigate the DSW ventilation rate, which is the volume flux of DSW exported from the continental shelf that ultimately produces CDBW, and thereafter the contribution of CDBW to total AABW. The annual transport of CDBW down Wild Canyon is estimated from mooring data at M3 to be 0.52 ± 0.26 Sv (Sv $= 10^6$ m^3 s^{-1}; Methods). In conjunction with another estimate using a salinity budget from satellite data, we propose that 0.3–0.7 Sv of DSW is ventilated in this region (Methods). This represents ~6–13% of the circumpolar contribution based on the total DSW ventilation rate of 5.4 Sv determined from chlorofluorocarbon data[38] and is of the same order of magnitude as DSW export reported from Adélie Land[14]. This significant surface-to-bottom injection is consistent with the local maxima of near-bottom chlorofluorocarbon and oxygen concentrations offshore and to the west of Cape Darnley, as shown in the detailed hydrographic atlas[20]. To examine how much WSDW is renewed through CDBW, we adopt the mean property of AABW in the Atlantic sector[2], which is close to that of WSDW (Supplementary Fig. S8a). Using the DSW ventilation rate estimated above and the mixing ratio of CDBW and CDW to this mean property, the contribution of CDBW is estimated to be 0.65–1.5 Sv (Methods). There have been several estimates[2,39,40] for total AABW production in the Atlantic sector, in the ~3–10 Sv range. Taking the well-referenced value of 4.9 Sv (ref. 2), the CDBW contribution is ~13–30% of the Atlantic AABW production.

In comparison to the other AABW formation regions, we note that the periodicity of the overflows is similar to that reported in the Weddell[32] and Ross[34] seas and the AABW layer thickness is comparable to that in the Ross Sea[11,12]. One difference is that the influence of tides is much weaker here (<0.05 m s^{-1}) relative to the Ross Sea[11,12]. Most importantly, the Cape Darnley region demonstrates conclusively that a relatively narrow section of continental shelf with limited DSW storage capacity can produce AABW from polynya-driven sea-ice production alone. We therefore speculate that there could be further AABW-formation discoveries in similar polynyas, particularly those in East Antarctica[15,25] (Supplementary Table S1).

High sea-ice production in the CDP results from Cape Darnley ice barrier (iceberg tongue) blocking the westward advection of sea ice. This mechanism is similar to that of the Mertz Glacier Tongue and Drygalski Ice Tongue on the Mertz and Terra Nova Bay polynyas, respectively. As demonstrated by the calving of Mertz Glacier Tongue in 2010, the rapid change (collapse) of such a barrier can cause a pronounced change in sea-ice and AABW production[41,42]. Although the iceberg tongue and sea-ice production in the CDP were relatively stable during the AMSR-E period from 2003 to 2010 (Supplementary Section S1), any significant change to the structure of the ice barrier would strongly impact CDBW production.

This study now raises the profile of CDBW to that of an important contributor to WSDW, a major component of the AABW driving the lower limb of the meridional overturning circulation (MOC) of the Atlantic Sector[43]. It has been reported that WSDW has been warming since the 1980s (ref. 44), with its volume possibly contracting[45], and that this could result in a weakening of the MOC. Furthermore, sediment-core records taken around the CDP indirectly suggest that there has been millennium-scale variability in the local AABW production[46]. It is vital that CDBW be incorporated into the global assessment of the MOC, a key element of the climate system. This will improve numerical simulations predicting its response to long-term climate change.

Methods

Estimation of the DSW ventilation rate. We make two estimates of the DSW ventilation rate. The first estimate is based on the transport of AABW down Wild Canyon using velocity and temperature data from M3 (Supplementary Section S5). New AABW is defined as water with potential temperature $\theta < -0.4$ °C, based on the bimodal distribution of near-bottom temperature that separates around −0.4 °C (Supplementary Fig. S7). The AABW layer

thickness and speed are inter/extra-polated from the available instrument range. The layer thickness and velocities from this single mooring provide the transport of new AABW (CDBW) per unit width (Fig. 2e). When the width of the downslope current is assumed to be 20 km based on the canyon width, the annual transport of CDBW is 0.52 ± 0.26 Sv. Using this transport, the DSW ventilation rate is estimated to be 0.30 ± 0.15 Sv on the assumption that CDBW ($\theta = -0.65\,^{\circ}C$, $S = 34.635$) is a 42:58 mixture of CDW ($\theta = 1.05\,^{\circ}C$, $S = 34.71$) to DSW ($\theta = -1.9\,^{\circ}C$, $S = 34.58$) from observed water properties (Supplementary Fig. S8a).

The second estimate of the DSW ventilation rate is based on a salt budget from sea-ice production (Supplementary Section S6b), where we assume that summer water masses are directly transformed into winter DSW by the salt flux from sea-ice production in the CDP. Using the annual sea-ice production derived from the satellite data and heat-flux calculation (Supplementary Fig. S2), the salt-budget calculation yields an annual DSW ventilation rate of 0.70 ± 0.25 Sv. The 0.30 Sv estimated from the CDBW transport down Wild Canyon represents a lower bound for the entire CDP region because there is further CDBW transport mainly down Daly Canyon. Meanwhile, the 0.70 Sv derived from the salt budget represents an upper bound, because the sea-ice production in the CDP does not directly equate to DSW formation and export for CDBW production.

Estimation of the CDBW contribution to AABW production. The AABW produced off the CDP (CDBW) is further mixed with overlying warmer water to become general AABW in the Weddell Sea. We evaluate the flux of CDBW that contributes to the final output of AABW in this sector. When the averaged property of AABW in the Atlantic sector[2] (mainly in the Weddell Sea; $\theta = -0.30\,^{\circ}C$, $S = 34.66$) is plotted in the θ–S diagram of Supplementary Fig. S8a, it is located near the mixing line linking DSW, CDBW and CDW. Assuming that CDBW is finally mixed with the CDW to become the averaged AABW, the mixing ratio of CDBW and CDW is calculated to be 79:21, based on θ. Using this mixing ratio and the estimated annual transport of CDBW down Wild Canyon (0.52 Sv), the ultimate contribution of CDBW to the AABW in the Weddell Sea would be 0.65 Sv. Further, if we use this mixing line and ratio for the original end point of DSW and apply them to the upper bound estimation of DSW from the sea-ice production, the ultimate contribution of CDBW would be 1.5 Sv ($=0.65 \times 0.7/0.3$ Sv).

Animal ethics. Animal ethics for all animal handling was approved by the University of Tasmania and Macquarie University's Animal Ethics Committees.

Received 25 June 2012; accepted 21 January 2013; published online 24 February 2013

References

1. Johnson, G. C. Quantifying Antarctic Bottom Water and North Atlantic Deep Water volumes. *J. Geophys. Res.* **113,** C05027 (2008).
2. Orsi, A. H., Johnson, G. C. & Bullister, J. L. Circulation, mixing, and production of Antarctic Bottom Water. *Prog. Oceanogr.* **43,** 55–109 (1999).
3. Marshall, J. & Speer, K. Closure of the meridional overturning circulation through Southern Ocean upwelling. *Nature Geosci.* **5,** 171–180 (2012).
4. Sigman, D. M. & Boyle, E. A. Glacial/interglacial variations in atmospheric carbon dioxide. *Nature* **407,** 859–869 (2000).
5. Baines, P. G. & Condie, S. in *Ocean, Ice, and Atmosphere: Interactions at the Antarctic Continental Margin* (eds Jacobs, S. & Weiss, R.) 29–49 (Antarct. Res. Ser., Vol. 75, American Geophysical Union, 1998).
6. Foster, T. D. & Carmack, E. C. Frontal zone mixing and Antarctic Bottom Water formation in the southern Weddell Sea. *Deep Sea Res. Oceanogr. Abstr.* **23,** 301–317 (1976).
7. Gordon, A. L., Huber, B. A., Hellmer, H. H. & Ffield, A. Deep and bottom water of the Weddell Sea's western rim. *Science* **262,** 95–97 (1993).
8. Fahrbach, E., Harms, S., Rohardt, G., Schröder, M. & Woodgate, R. A. Flow of bottom water in the northwestern Weddell Sea. *J. Geophys. Res.* **106,** 2761–2778 (2001).
9. Foldvik, A. *et al.* Ice shelf water overflow and bottom water formation in the southern Weddell Sea. *J. Geophys. Res.* **109,** C02015 (2004).
10. Jacobs, S. S., Amos, A. F. & Bruchhausen, P. M. Ross Sea oceanography and Antarctic Bottom Water formation. *Deep-Sea Res. Oceanogr. Abstr.* **17,** 935–970 (1970).
11. Whitworth, T. III & Orsi, A. H. Antarctic bottom water production and export by tides in the Ross Sea. *Geophys. Res. Lett.* **33,** L12609 (2006).
12. Gordon, A. L. *et al.* Western Ross Sea continental slope gravity currents. *Deep-Sea Res. II* **56,** 796–817 (2009).
13. Rintoul, S. R. in *Ocean, Ice, and Atmosphere: Interactions at the Antarctic Continental Margin* (eds Jacobs, S. & Weiss, R.) 151–171 (Antarct. Res. Ser., Vol. 75, American Geophysical Union, 1998).
14. Williams, G. D., Bindoff, N. L., Marsland, S. J. & Rintoul, S. R. Formation and export of dense shelf water from the Adélie Depression, East Antarctica. *J. Geophys. Res.* **113,** C04039 (2008).
15. Williams, G. D. *et al.* Antarctic Bottom Water from the Adélie and George V Land coast, East Antarctica (140–149° E). *J. Geophys. Res.* **115,** C04027 (2010).
16. Jacobs, S. S. & Georgi, D. T. in *A voyage of discovery* (ed. Angel, M.) 43–84 (Pergamon Press, 1977).
17. Mantisi, F., Beauverger, T., Poisson, A. & Metzl, N. Chlorofluromethanes in the western Indian sector of the Southern Ocean and their relations with geochemical tracers. *Mar. Chem.* **35,** 151–167 (1991).
18. Meredith, M. P. *et al.* On the sources of Weddell Gyre Antarctic Bottom Water. *J. Geophys. Res.* **105,** 1093–1104 (2000).
19. Hoppema, M. *et al.* Prominent renewal of Weddell Sea Deep Water from a remote source. *J. Mar. Res.* **59,** 257–279 (2001).
20. Orsi, A. H. & Whitworth, T. III in *Hydrographic Atlas of the World Ocean Circulation Experiment (WOCE). Volume 1: Southern Ocean* (eds Sparrow, M., Chapman, P. & Gould, J.) (International WOCE Project Office, 2005).
21. Meijers, A. J. S., Klocker, A., Bindoff, N. L., Williams, G. D. & Marsland, S. J. The circulation and water masses of the Antarctic shelf and continental slope between 30 and 80° E. *Deep-Sea Res. II* **57,** 723–737 (2010).
22. Middleton, J. H. & Humphries, S. E. Thermohalinestructure and mixing in the region of Prydz Bay, Antarctica. *Deep-Sea Res.* **36,** 1255–1266 (1989).
23. Nunes Vaz, R. A. & Lennon, G. W. Physical oceanography of the Prydz Bay region of Antarctic waters. *Deep-Sea Res. I* **43,** 603–641 (1996).
24. Yabuki, T. *et al.* Possible source of the Antarctic Bottom Water in the Prydz Bay region. *J. Oceanogr.* **62,** 649–655 (2006).
25. Tamura, T., Ohshima, K. I. & Nihashi, S. Mapping of sea-ice production for Antarctic coastal polynyas. *Geophys. Res. Lett.* **35,** L07606 (2008).
26. Fedak, M.A. Marine mammals as platforms for oceanographic sampling: A win/win situation for biology and operational oceanography. *Mem. Natl Inst. Polar Res.* **58,** 133–147 (2004).
27. Charrassin, J-B. *et al.* Southern Ocean frontal structure and sea-ice formation rates revealed by elephant seals. *Proc. Natl Acad. Sci. USA* **105,** 11634–11639 (2008).
28. Williams, G. D. *et al.* Upper ocean stratification and sea ice growth rates during the summer-fall transition, as revealed by Elephant seal foraging in the Adélie Depression, East Antarctica. *Ocean Sci.* **7,** 185–202 (2011).
29. Massom, R. A., Harris, P. T., Michael, K. J. & Potter, M. J. The distribution and formative processes of latent-heat polynyas in East Antarctica. *Ann. Glaciol.* **27,** 420–426 (1998).
30. Fraser, A. D., Massom, R. A., Michael, K. J., Galton-Fenzi, B. K. & Lieser, J. L. East Antarctic landfast sea-ice distribution and variability, 2000–2008. *J. Clim.* **25,** 1137–1156 (2012).
31. Matsumura, Y. & Hasumi, H. Modeling ice shelf water overflow and bottom water formation in the southern Weddell Sea. *J. Geophys. Res.* **115,** C10033 (2010).
32. Darelius, E., Smedsrud, L. H., Østerhus, S., Foldvik, A. & Gammelsrød, T. Structure and variability of the Filchner overflow plume. *Tellus Ser. A* **61,** 446–464 (2009).
33. Wang, Q., Danilov, S. & Schröter, J. Bottom water formation in the southern Weddell Sea and the influence of submarine ridges: Idealized numerical simulations. *Ocean Model.* **28,** 50–59 (2008).
34. Budillon, G., Castagno, P., Aliani, S., Spezie, G. & Padman, L. Thermohaline variability and Antarctic bottom water formation at the Ross Sea shelf break. *Deep-Sea Res. I* **58,** 1002–1018 (2011).
35. Roquet, F. *et al.* Delayed-mode calibration of hydrographic data obtained from animal-borne satellite relay data loggers. *J. Atmos. Ocean. Technol.* **41,** 787–801 (2011).
36. Gordon, A. L., Visbeck, M. & Huber, B. Export of Weddell Sea Deep and Bottom Water. *J. Geophys. Res.* **106,** 9005–9017 (2001).
37. Orsi, A. H. & Wiederwohl, C. L. A recount of Ross Sea waters. *Deep-Sea Res. II* **56,** 778–795 (2009).
38. Orsi, A. H., Smethie, W. M. Jr & Bullister, J. L. On the total input of Antarctic waters to the deep ocean: A preliminary estimate from chlorofluorocarbon measurements. *J. Geophys. Res.* **107,** 3122 (2002).
39. Meredith, M. P., Watson, A. J., van Scoy, K. A. & Haine, T. W. N. Chlorofluorocarbon-derived formation rates of the deep and bottom waters of the Weddell Sea. *J. Geophys. Res.* **106,** 2899–2919 (2001).
40. Naveira Garabato, A. C., McDonagh, E. L., Stevens, D. P., Heywood, K. J. & Sanders, R. J. On the export of Antarctic Bottom Water from the Weddell Sea. *Deep-Sea Res. II* **49,** 4715–4742 (2002).
41. Kusahara, K., Hasumi, H. & Williams, G. D. Impact of Mertz Glacier Tongue calving on dense shelf water. *Nature Commun.* **2,** 159 (2011).
42. Tamura, T., Williams, G. D., Fraser, A. D. & Ohshima, K. I. Potential regime shift in decreased sea ice production after the Mertz Glacier calving. *Nature Commun.* **3,** 826 (2012).

43. Meredith, M. P., Naveira Garabato, A. C., Gordon, A. L. & Johnson, G. C. Evolution of the deep and bottom waters of the Scotia Sea, Southern Ocean, during 1995–2005. *J. Clim.* **21,** 3327–3343 (2008).
44. Fahrbach, E. *et al.* Warming of deep and abyssal water masses along the Greenwich meridian on decadal time scales: The Weddell gyre as a heat buffer. *Deep-Sea Res. II* **58,** 2508–2523 (2011).
45. Purkey, S. G. & Johnson, G. C. Global contraction of Antarctic Bottom Water between the 1980s and 2000s. *J. Clim.* **25,** 5830–5844 (2012).
46. Harris, P. T. Ripple cross-laminated sediments on the East Antarctic Shelf: Evidence for episodic bottom water production during the Holocene? *Mar. Geol.* **170,** 317–330 (2000).

Acknowledgements

We are deeply indebted to the officers, crew and scientists on board TR/V *Umitaka-maru* and R/V *Hakuho-maru* for their help with field observations. Comments by R. A. Massom and support from K. Shimada and K. Kitagawa were helpful. The AMSR-E and SSM/I data were provided by the National Snow and Ice Data Center (NSIDC), University of Colorado. The ASAR data were provided by European Space Agency. IMOS seal CTD data were provided through the Australian Animal Tracking and Monitoring System, a facility of Integrated Marine Observing System. Isles Kerguelen deployments were supported by the French Spatial Agency (CNES) and the French Polar Institute (IPEV). This work was supported by Grants-in-Aids for Scientific Research (20221001, 20540419, 21740337, 23340135) of the Ministry of Education, Culture, Sports, Science and Technology in Japan, and the Australian Government's Cooperative Research Centres Programme through the Antarctic Climate & Ecosystem Cooperative Research Centre.

Author contributions

K.I.O. and Y.F. conducted and analysed mooring observations after planning the experiment with M.W., S.A. and T.T. G.D.W. led the investigation of seal data with calibration by F.R., analysis by L.H-B., and fieldwork by I.F. and M.H. S.N. and T.T. analysed satellite data. Y.K. and D.H. conducted hydrographic observations.

Additional information

Supplementary information is available in the online version of the paper. Reprints and permissions information is available online at www.nature.com/reprints. Correspondence and requests for materials should be addressed to K.I.O.

Competing financial interests

The authors declare no competing financial interests.